Analysis of Permanent Magnet Type Transverse Flux Linear Motor by Coupling 2D Finite Element Method on 3D Equivalent Magnetic Circuit Network Method

Ji-Young Lee, and Jung-Pyo Hong
Dept. of Electrical Engineering
Changwon National University
Changwon, Korea
jyecad@korea.com

Do-Hyun Kang
Mechatronics Research Group
Korea Electrotechnology Research Institute
Changwon, Korea
dhkang@keri.re.kr

Abstract— **Permanent Magnet (PM) type Transverse Flux Linear Motors (TFLMs) are electromagnetic devices which can develop directly powerful linear motion. The unique configuration makes the output power higher than longitudinal motors, but also it makes characteristic analyses difficult. This paper deals with an effective analysis of a PM type TFLM by coupling 2-dimensional Finite Element Method (2D FEM) on 3D Equivalent Magnetic Circuit Network Method (EMCN). 2D analysis by FEM is used to find so-called Multiple-ratio, which is multiplied by 3D analysis results, and 3D EMCN is employed in magnetic field analysis to get the static thrust and parameters for system assessment such as flux linkage, co-energy, apparent inductance, and incremental inductance. The calculated results are verified by comparison with measurements.**

Keywords-component; Permanent Magnet, 3D Equivalent Magnetic Circuit Network Method, Transverse Flux Linear Motor, 2D Finite Element Method.

I. INTRODUCTION

Linear motors are electromagnetic devices developing mechanical thrust without gear or rotary-to-linear converters. The advantages of linear motors include low noise, reduced operating cost, and increased flexibility of operation because of the gearless feature. Linear motors, however, have a few practical limitations. The major reason is the low power density due to the inherent large air gap [1]. For the application of linear motors to high power system, therefore, Permanent Magnet (PM) type Transverse Flux Linear Motors (TFLMs) can be considered because the motors can develop high magnetic thrust and reluctance thrust in relatively small air gap. There are several practical examples of TFLMs and their rotary counterparts in [2]-[5].

The design and analysis of TFLMs require analytical models for performance assessment and system simulation. To get the parameters of the analytical models such as flux and inductance, it is required to employ 3-dimensional (3D) analysis because of the magnetically complicated and nonsymmetrical configuration. Despite of 3D analysis, the analysis of TFLMs sometimes can be more difficult than that of rotary counterparts, or the results can be inaccurate because of the end effect by limited mover length.

Therefore, this paper deals with an analysis method of a PM type TFLM for an electro-dynamic vibrator by coupling 2D Finite Element Method (FEM) on 3D Equivalent Magnetic Circuit Network Method (EMCN).

To estimate the performance of vibrator, the static thrust, flux linkage, apparent and incremental inductances are calculated by 3D EMCN. For TFLM as a linear motor, the analysis method is more useful and proper than 3D FEM because of the hexahedral elementary shape and relatively fast solving time [6], [7].

Since the vibrator is too long to model whole shape considering analysis time and accuracy, the portion of two stator-pole pitches is taken as the 3D analysis model. By the model, however, end effect at the mover-end cannot be considered so that so-called Multiple-ratio is needed to be multiplied by the 3D analysis results as a kind of an adjustment factor. This ratio can be obtained by the analysis of 2D model with imaginary magnetic flux path [4] for considering the 3D flux path of TFLM. The 2D analysis model does not need to have the whole shape of the actual model. It is enough to model the mover and a little longer stator which is long enough to consider the mover-end leakage flux. The Multiple-ratio is not equal to either length ratio or pole ratio of analysis model to actual model.

After calculating magnetic characteristics of the vibrator from the analysis results by 2D FEM and 3D EMCN, flux linkage and inductances are adjusted by stator end-coil leakage component computed by experimental equation [8]. Among these analysis results, thrust and apparent inductance are compared with the measurements to verify the analysis results.

II. BASIC CONFIGURATIONS OF TFLM

Depending on the excitation, there are two distinct configurations of TFLMs as follows [10].

(1) Electrically excited (TFE-LM)

(2) Magnetically excited (TFM-LM)

The basic configuration of the TFE-LM is presented in Fig.1 in comparison with a Longitudinal Flux Linear Motor (LFLM). The primary magnetic flux of TFE-LM flows

perpendicularly to the moving direction while the flux of LFLM does parallel to the moving direction. The moveable part of the TFE-LM is electrical passive and the thrust is generated based on the reluctance principle. When the primary windings are excited, the primary and secondary teeth align in opposite position.

The configuration of TFM-LM, so-called PM type TFLM in this paper, and the principles of force generation are shown in Fig. 2. The stator base irons are cut and developed to show the principles of force generation. The magnetic polarities between mover and stator generate the total thrust *Ft* in one direction. The PM type TFLM uses the PMs as excitation so that the magnetic flux density in the air gap can be amplified because the profile of the PM is bigger than the stator pole width in the air gap.

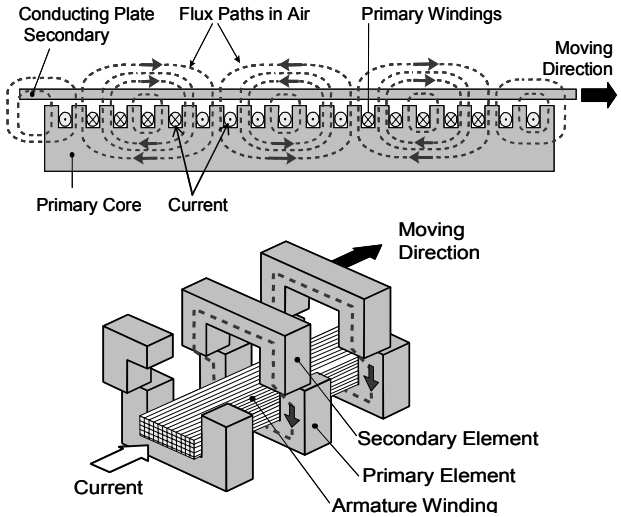

Figure 1. Longitudinal (upper) and transverse flux (lower) linear motor

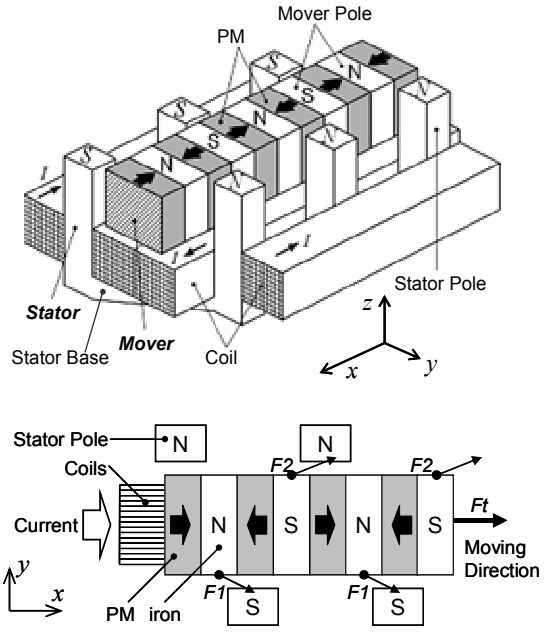

Figure 2. Configurations of PM type TFLM

III. Analysis Object

Fig. 3 shows the stator and the mover of TFLM which is fabricated for a two-phase electro-dynamic vibrator. The 3D configuration for one phase is identical to the configuration shown in Fig. 2. In this type of TFLM, the high power density is mainly due to high-energy PM and the saliency of mover. This principle is similar to spoke magnet type brushless motor [11]. In addition, it can have relatively small air gap because the attraction force can be compensated in two air gap.

Table 1 shows the specifications. The rated frequency is 4(Hz), and thrust force is 500(N). The more detail explanation about the phase arrangement and winding magnetomotive force (*mmf*) excitation principle of this vibrator are presented in [5].

Fig. 4 briefly shows the top view of the shape of one phase. The winding has two ring-shaped coils in series, and each coil is divided into three parts for analysis because the coil is too long to model the whole shape. Pt_M is the coil portion where the main flux exists and thrust occurs. Pt_L is the portion where leakage flux exists, and Pt_E is the end coil portion. The $2\tau_p$ of the two stator-pole pitch in Pt_M is the length of the 3D analysis model. The analysis results (thrust, flux, inductance etc.) obtained by each 3D model for Pt_M and Pt_L are multiplied by the each Multiple-ratio and adjusted by stator end-coil leakage component considering the portion Pt_E.

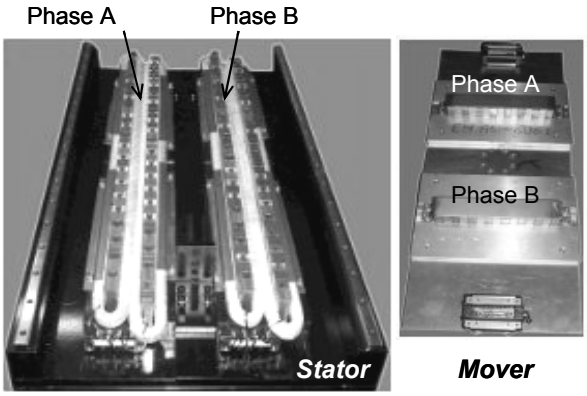

Figure 3. Fabrication of PM type TFLM

TABLE 1. SPECIFICATIONS PER ONE PHASE

Stator	***No. of Pole***	20	Pair
	No. of turn	140	Turn
	Rated Current	20	A
	Material	50A445 (M27)	
Mover	***No. of Pole***	7	
	Permanent Magnet	Br =1.2 μ_r =1.05	T
	Material	50A760 (M45)	
Air gap Length		0.7	mm
Rated Frequency		4	Hz
Rated Thrust		500	N

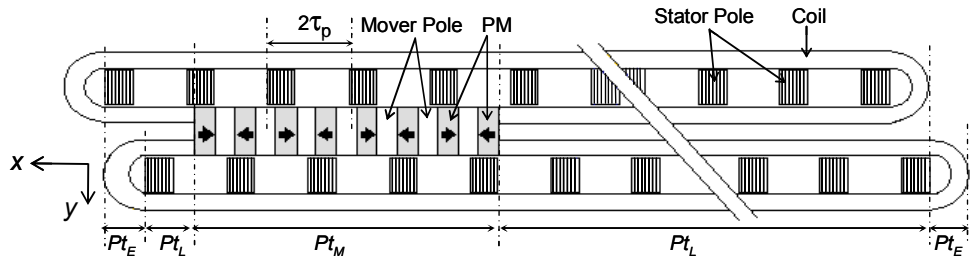

Figure 4. The top view for one phase of the TFLM

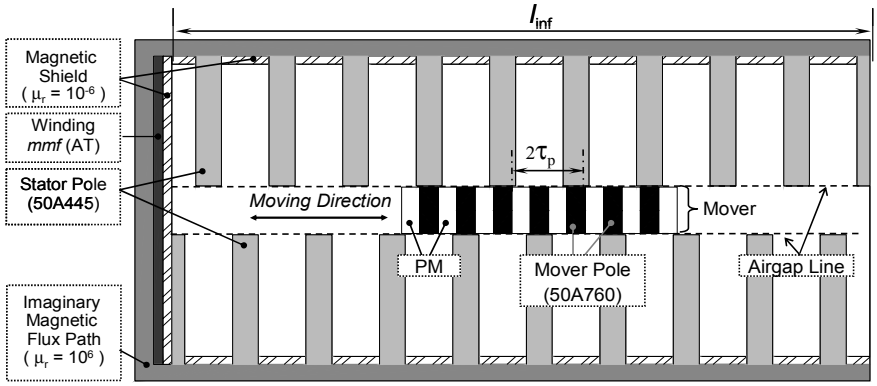

Figure 5. 2D analysis model with imaginary magnetic flux path

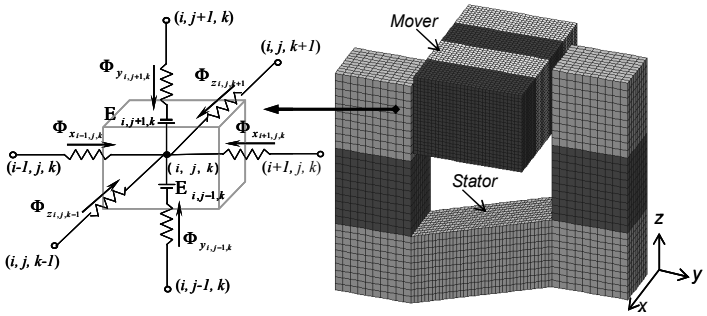

Figure 6. Conceptual model of one node in EMCN and meshed model

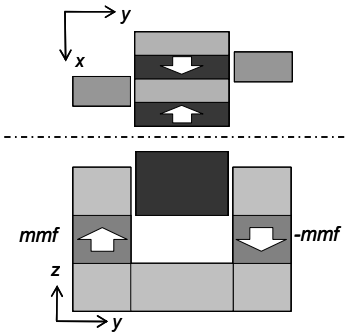

Figure 7. Magnetomotive force direction

IV. Analysis and Measurement Method

A. 2D Analysis by FEM

As the field variable of 2D FEM, vector potential is used in this paper, and to consider the end effect of mover and find the Multiple-ratio, 2D analysis model is constructed as shown in Fig. 5. While the 3D analysis model just reflects the original shape of the object, 2D analysis model needs more imaginary path to consider 3D magnetic flux path. For this TFLM analysis model, magnetic shield and imaginary magnetic flux path are substitutes for Stator Base actually having 3D flux path as shown in Fig. 2. Consequently the permeability of magnetic shield is about 0, and that of imaginary magnetic flux path is 10^6 as meaning of infinity. These two regions are analyzed by linear solution to keep the permeability constant in magneto-static field when the other regions are analyzed by nonlinear solution.

In 2D analysis model, current source is enclosed with the imaginary magnetic flux path and magnetic shield to make uniform magnetic flux between opposite side stator poles.

After solving the model, the Multiple-ratio is obtained by the ratio of thrust in $2\tau_p$ to in l_{inf} along the air gap line.

B. 3D Analysis by EMCN

3D EMCN is a numerical analysis technique that uses scalar potential as a field variable. For using this analysis method, the analysis model is divided into hexahedral shape elements according to regions. 3D EMCN is constructed by connecting the nodes of adjacent elements through permeance. The conceptual model about one node and 3D analysis model are given in Fig. 6. Magnetic flux continuity has a condition that the inflow of flux is equal to the outflow of flux at node (i, j, k). From magnetic flux continuity condition as (1), system matrix (2) is constructed using equivalent magnetomotive

force, *mmf,* of element in magnet source region which has linear demagnetization curve and in stator current. The magnetomotive force directions of analysis model are shown in Fig. 7.

$$\sum_{n=1}^{6}\Phi_n = \Phi_{1i,j,k} + \Phi_{2i,j,k} + \Phi_{3i,j,k} + \Phi_{4i,j,k} + \Phi_{5i,j,k} + \Phi_{6i,j,k} = 0 \quad (1)$$

$$[\mathbf{P}]\{\mathbf{U}\} = \{\mathbf{F}\} \quad (2)$$

where, Φ_n is the flux of nth element, [**P**] is permeance coefficient matrix, {**U**} is matrix of node magnetic scalar potential, and {**F**} is forcing matrix [6][7].

C. Inductance Calculation Method

The calculation process with the three models for apparent and incremental inductances is shown in Fig. 8. The two inductances are calculated by sum of inductances of each part.

The analysis model Pt_M has PMs in mover so that magnetic circuit can be saturated according to the mover position even if current is zero. Therefore, the apparent inductance is bigger than the incremental inductance, and the two inductances should be calculated by different methods in this region. In Pt_L, however, there is only leakage inductance. Since the region is hardly saturated due to its structure, the magnetic material maintains the linear characteristics even at maximum current. Therefore, the apparent and incremental inductances become identical, and both of the inductances can be calculated by either of two methods used for calculating inductances in Pt_M. In the end coil, the leakage inductance is small enough to be ignored generally, and the magnetic flux cannot be saturated in this part. Therefore, experimental equation can be used according to the coil shape, and added to both apparent and incremental inductances.

1) Apparent inductance

The process of calculation of apparent inductance using 3D EMCN is given below:

Step 1: The permeability of each element is obtained and saved at operating point for current variation by nonlinear analysis.

Step 2: To estimate the self-inductance of winding as apparent inductance, linear analysis is performed while keeping the magnetomotive force of PM to zero.

Step 3: Since the three inductances, incremental, apparent, and effective inductances, are identical in linear system, the apparent inductance is calculated by the effective inductance equation [7].

2) Incremental inductance

Since salient pole machines with concentrated windings have so small mutual inductance that it can be neglected, the voltage equation of a phase is represented as (3). For the TFLM, the voltage equation also can be described by (3) because the mover has doubly salient pole structure due to the arrangement of PMs and iron poles, and it has the concentrated windings in stator. In this equation, magnetic flux linkage λ is the function of phase current i, and mover position x. L_{inc} denotes the incremental inductance.

$$V = iR + \frac{d\lambda}{dt} = iR + \frac{\partial\lambda}{\partial i}\frac{\partial i}{\partial t} + \frac{\partial\lambda}{\partial x}\frac{\partial x}{\partial t}$$
$$= iR + L_{inc}\frac{di}{dt} + \frac{\partial\lambda}{\partial x}\frac{dx}{dt} \quad (3)$$

where V is terminal voltage and R is phase resistance. Incremental inductance is calculated by the definition of (3). According to input current variation, flux linkage is obtained as one of 3D analysis results.

3) Experimental equation

Simple experimental equations are introduced in [8] and [9], and this paper uses one in [8] for the end coil inductance $L_{end.}$ The equation is as following.

$$L_{end} = 0.002\pi^2 a\left(\frac{2a}{b}\right)N^2 K \quad (\mu H) \quad (4)$$

where a is coil radius, b is coil length, N is the number of turn, and K is Nagaoka's coefficient.

D. Test method

In the test for inductance measurement using AC power supply, the inductance is actually calculated by measured voltage V_{rms}, current I_{rms} and phase angle θ using (5).

$$R = \frac{V_{rms}\cos\theta}{I_{rms}}, \qquad L = \frac{V_{rms}\sin\theta}{\omega I_{rms}} = \frac{V_{rms}\sin\theta}{2\pi f\, I_{rms}} \quad (5)$$

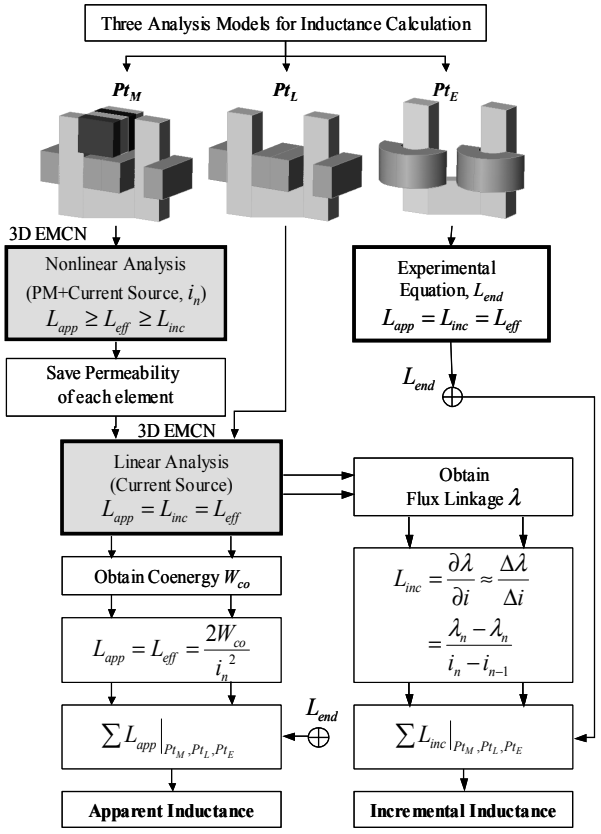

Figure 8. Inductance calculation process of TFLM

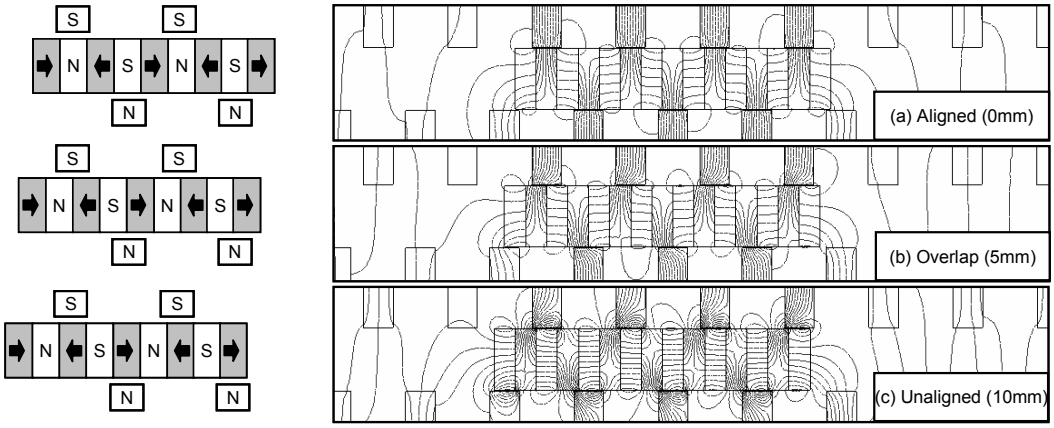

Figure 9. The top view for one phase of the TFLM

TABLE II. THE MULTIPLE-RATIO OF ANALYSIS MODEL TO ACTUAL MODEL

	3D EMCN Model Length	Actual Model Length	Length-ratio	Multiple-ratio
Pt_M	40 mm	150 mm	3.75	3.6
Pt_L	40 mm	714 mm	17.85	17.5

V. ANALYSIS AND MEASUREMENT RESULTS

A. 2D Analysis Results

Fig. 9 and Fig. 10 show the 2D analysis results by FEM. 0(mm) is the base position where mover and stator poles are aligned. Fig. 9 presents the variation of equi-potential line for mover displacement, and it shows the influence of mover-end leakage flux. Fig. 10 is thrust for *mmf* and integral path variation. The $2\tau p$ is the 3D analysis model length, and l_{inf} is the integral length where the thrust does not change any more over mover length. The Multiple-ratio in Pt_M is calculated by the ratio of thrust for $2\tau p$ to thrust for l_{inf}.

The Multiple-ratio in Pt_L is calculated by the ratio of the length for $2\tau p$ to the length obtained by subtracting l_{inf} from winding length because leakage flux of stator coil is proportional to the integral length in this region. The calculated results of Multiple-ratio are in Table 2.

B. 3D Analysis Results

Thrust and the characteristic parameters such as flux and inductances are calculated by 3D EMCN, and multiplied by the Multiple-ratio in Table 2.

Fig. 11 shows the thrust developed by one phase according to current variation and mover displacement. Since the input current is considered to have ideal rectangular shape, these thrust values can be compared with static thrust measured under constant current condition. Flux linkage at all stator poles are shown in Fig. 12. With these flux data, incremental inductance can be calculated using (3).

Fig. 13 to Fig. 15 show the calculated inductances. The total apparent inductance shown in Fig. 14 is obtained by summing each inductance of three parts as shown in Fig. 13, and the total incremental inductance shown in Fig. 15 is obtained by the flux in Fig. 12. While the incremental inductance is the important parameter for system simulation, the apparent inductance is the parameter that can be compared to the value of measurement.

C. Comparisons with Analysis and Measurement Results

Computed thrust and apparent inductance are compared with measurements in Fig. 16 and Fig. 17. The comparison of thrusts shows a good agreement.

In the comparison of inductances, however, the average errors are about 7.5% and 6% for 2A and 4A respectively. The reason for error can be explained by the fact that the test is accomplished with 60Hz AC current whereas the frequency is not considered in analysis. While the electrical motors with large air-gap have constant inductance according to frequency, the motors with small air-gap can have variable inductance, which is decreased as frequency increases. As one example, the experimental results with LCR meter are shown in Fig. 11 under no-load condition. If the frequency is kept lower even under load condition, the error could be reduced to less than 5%.

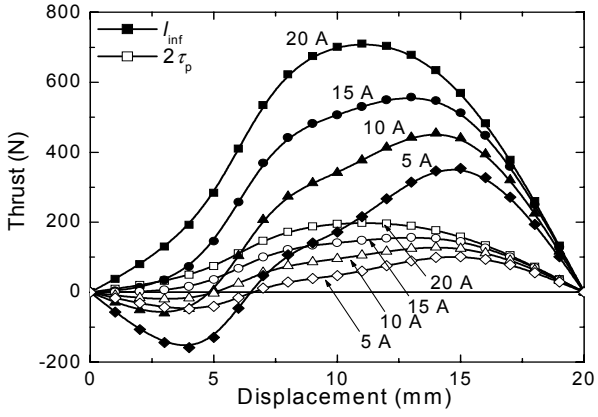

Figure 10. Thrust for input current and integral length

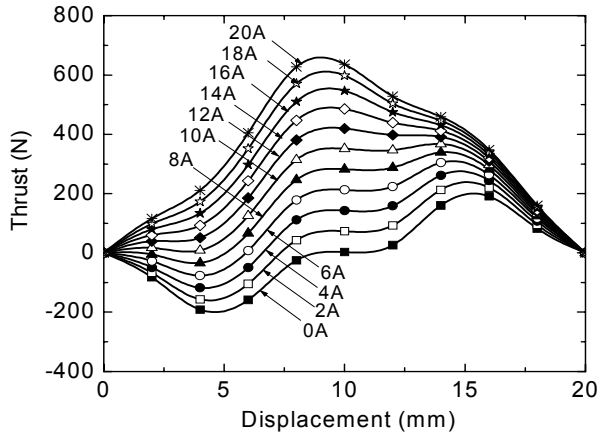

Figure 11. Thrust per one phase for current variation

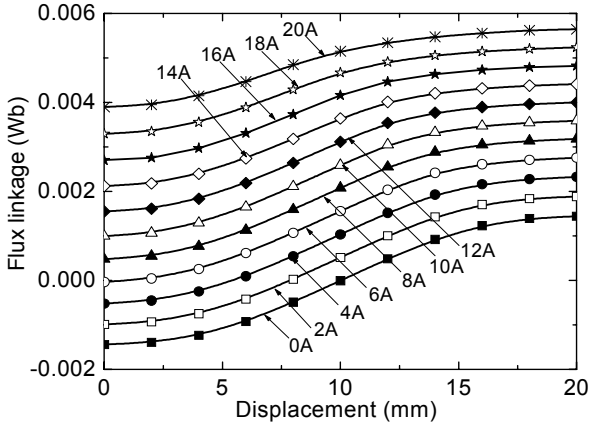

Figure 12. Flux linkage per one turn for current variation

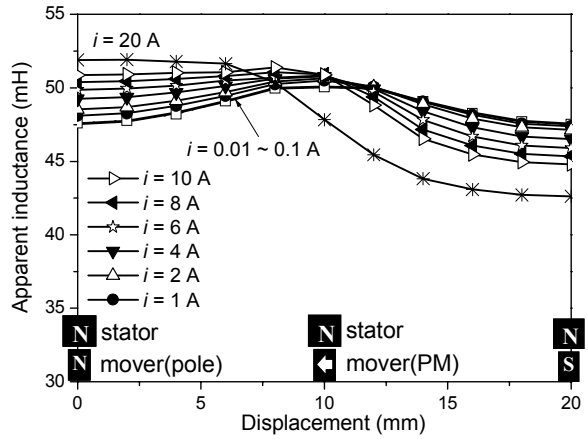

Figure 14. Total apparent inductance for current variation

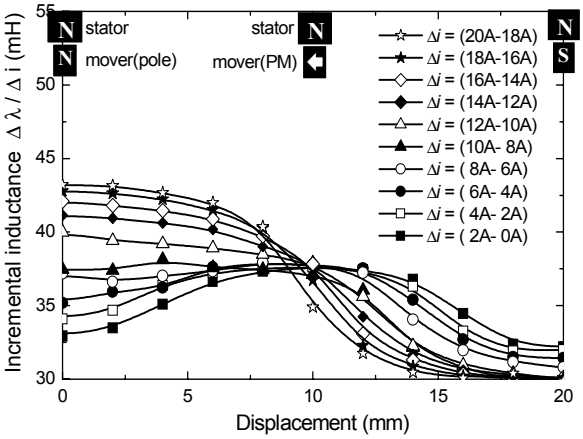

Figure 15. Total incremental inductance for current variation

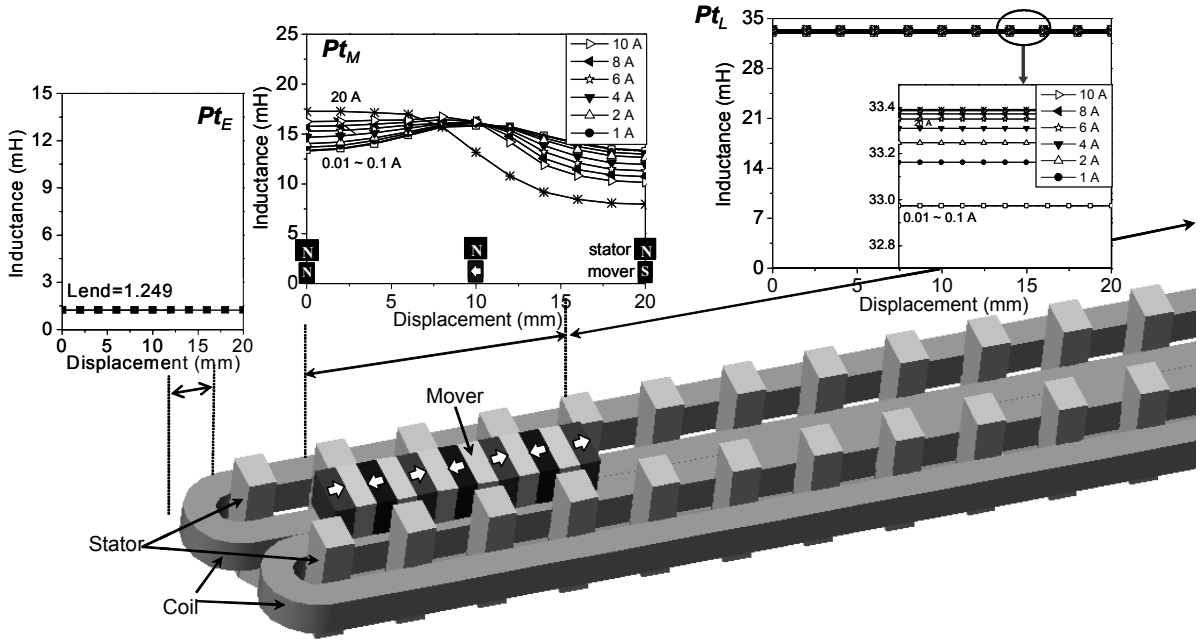

Figure 13. Apparent inductances of each part, Pt_E, Pt_M, and Pt_L

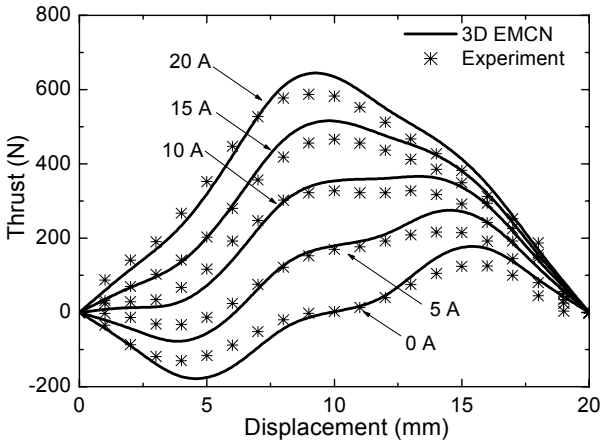

Figure 16. Comparison of thrusts for current variation

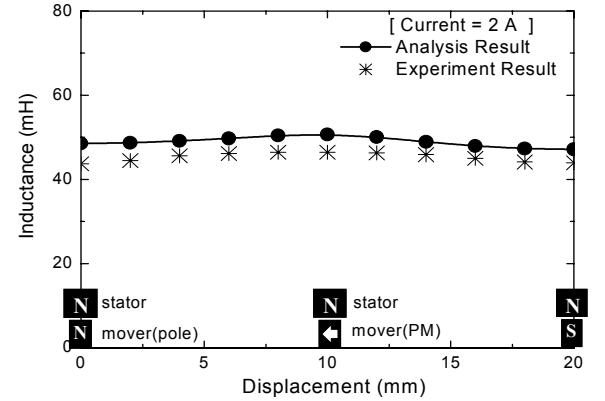

(a) Input current = 2A

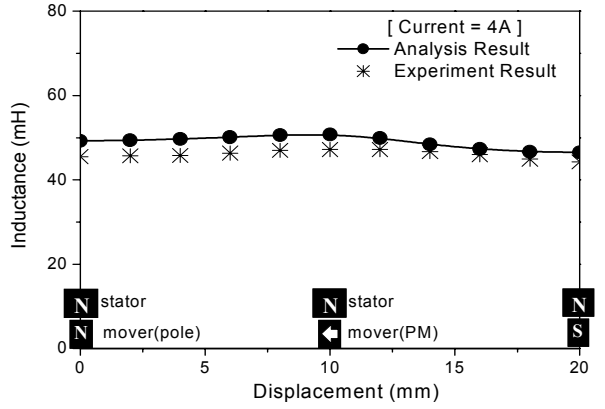

(b) Input current = 4A

Figure 17. Comparison of calculated and experimental inductances

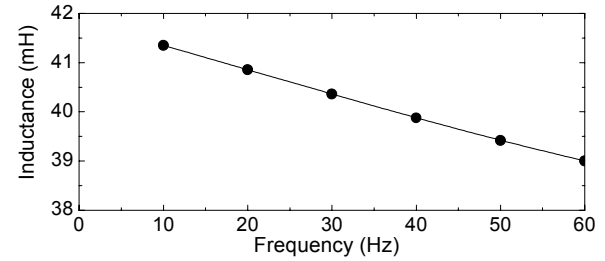

Figure 18. Inductance drop according to frequency under no-load condition

VI. CONCLUSIONS

In this paper, the effective method and the process for PM type TFLM analysis are introduced. Considering the length of the machine, the analysis model is divided into three portions. The static thrust and parameters, such as flux and inductances, are computed from 3D EMCN for each portion, and then each value is multiplied by Multiple-ratio obtained by 2D FEM. The calculation results are compared with the measurements, and the comparison shows the validity of the calculation method. Therefore, it is expected that the computed results (flux, inductances, etc.) in this research can be used as reliable parameters in dynamic simulation to estimate the performance, and the static thrust can also be the reference data for design of PM type TFLM. This analysis can be an essential process to apply TFLM to various field of industry as a linear actuator.

ACKNOWLEDGMENT

This work was financially supported by MOCIE through IERC program, Korea

REFERENCES

[1] Syed A. Nasar and I. Boldea, Linear Electric Motors: Theory, Design, and Practical Applications, Prentice-Hall, Inc.

[2] Mitcham, A.J., "Transverse flux motors for electric propulsion of ships," IEE Colloquium, New Topologies for Permanent Magnet Machines, pp. 3/1-3/6, 1997

[3] Andrzej M. Pawlak, Steven Schultz, and Vineeta Gangla, "Rotary Actuators with Mulitipole Ring Magnets," IEEE Trans., Industry Applications, Vol. 31, No. 6, pp1306-1314, 1995

[4] Do Hyun Kang, Yeon Ho Jeong, Moon Hwan Kim, " A study on the design of transverse flux linear motor with high power density," IEEE International symposium, Industrial Electronics 2001 Proceedings, Vol. 2, No. 3, pp707-711, 2001

[5] Tae-yun Lim, Do-Hyun Kang, Jong-Moo Kim, and Dong-Hee Kim, " A Study on control of drive for Vibrator Using PM-type Transverse Flux Linear Motor," Proceedings of the Power Conversion Conference-Osaka 2002, Vol. 1, pp43-47, 2002

[6] Jin Hur, Dong-Seok Hyun, and Jung-Pyo Hong, "A Method for Recuction of Cogging Torque in Brushless D.C. Motor Considering the Ditribution of Magnetization by 3DEMCN," IEEE Trans., Magnetics, Vol.34, No.5, pp.3532-3535, September, 1998

[7] Jin Hur, In-Soung Jung, and Dong-Seok Hyun, "Lateral Characteristic Analysis of PMLSM Considering Overhang Effect by 3 Dimensional Equivalent Magnetic Circuit Network Method," IEEE Trans., Magnetics, Vol. 34, No. 5, pp.3528-3531, September, 1998

[8] Frederick W. Grover, "Inductance Calculations," D. Van Nostrand Company, Inc.

[9] TJE Miller, *SPEED Consortium PC-SRD version7.0 Uwer's Manual*, University of Glasgow, June 1999

[10] D. H. Kang, Y. H. Chun, and H. Weh, "Analysis and optimal design of transverse flux linear motor with PM excitation for railway traction," IEE Proc. Electr. Power Appl. Vol. 150, No. 4, pp493-499, July, 2003

[11] J.R. Hendershot Jr, and T. J. E. Miller, Design of Brushless Permanent-Magnet Motors, Magna Physics Publishing and Clarendon Press, Oxford, 1994